AD-A139 116 TWO METHODS FOR CALCULATING THE PHYSICAL OPTICS FIELD 1/1
(U) NAVAL RESEARCH LAB WASHINGTON DC W B GORDON
29 FEB 84 NRL-MR-5289

UNCLASSIFIED F/G 12/1 NL

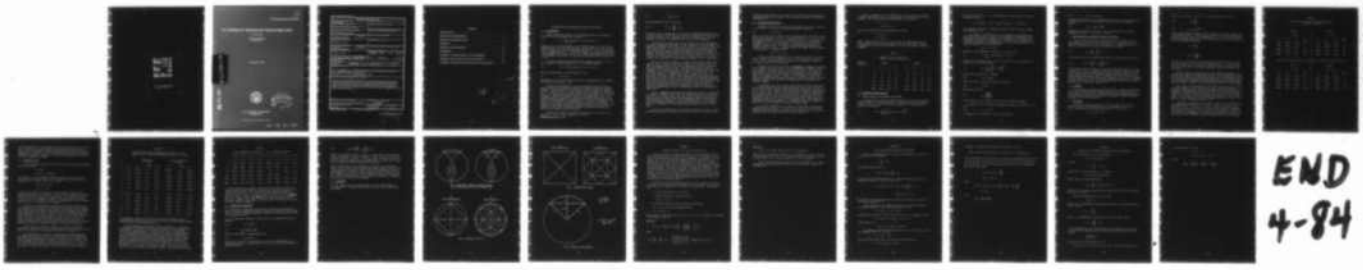

END
4-84

NRL Memorandum Report 5289

Two Methods for Calculating the Physical Optics Field

W. B. GORDON

Radar Analysis Branch
Radar Division

February 29, 1984

NAVAL RESEARCH LABORATORY
Washington, D.C.

SECURITY CLASSIFICATION OF THIS PAGE

REPORT DOCUMENTATION PAGE

1a. REPORT SECURITY CLASSIFICATION UNCLASSIFIED	1b. RESTRICTIVE MARKINGS
2a. SECURITY CLASSIFICATION AUTHORITY	3. DISTRIBUTION/AVAILABILITY OF REPORT Approved for public release; distribution unlimited.
2b. DECLASSIFICATION/DOWNGRADING SCHEDULE	
4. PERFORMING ORGANIZATION REPORT NUMBER(S) NRL Memorandum Report 5289	5. MONITORING ORGANIZATION REPORT NUMBER(S)
6a. NAME OF PERFORMING ORGANIZATION Naval Research Laboratory 6b. OFFICE SYMBOL (If applicable)	7a. NAME OF MONITORING ORGANIZATION
6c. ADDRESS (City, State and ZIP Code) Washington, DC 20375	7b. ADDRESS (City, State and ZIP Code)
8a. NAME OF FUNDING/SPONSORING ORGANIZATION Office of Naval Research 8b. OFFICE SYMBOL (If applicable)	9. PROCUREMENT INSTRUMENT IDENTIFICATION NUMBER
8c. ADDRESS (City, State and ZIP Code) Arlington, VA 22217	10. SOURCE OF FUNDING NOS. PROGRAM ELEMENT NO.: 61153N PROJECT NO.: RR0210541 TASK NO.: WORK UNIT NO.: 53-0626-0-0
11. TITLE (Include Security Classification) TWO METHODS FOR CALCULATING THE PHYSICAL OPTICS FIELD	
12. PERSONAL AUTHOR(S) W. B. Gordon	
13a. TYPE OF REPORT Interim 13b. TIME COVERED FROM 10/82 TO 9/83	14. DATE OF REPORT (Yr., Mo., Day) February 29, 1984 15. PAGE COUNT 23
16. SUPPLEMENTARY NOTATION	
17. COSATI CODES FIELD / GROUP / SUB. GR.	18. SUBJECT TERMS (Continue on reverse if necessary and identify by block number) Physical Optics Electromagnetic scattering

19. ABSTRACT (Continue on reverse if necessary and identify by block number)

In the theory of Physical Optics the field scattered by a curved reflecting surface S is represented by an integral whose numerical evaluation is difficult. Two methods for calculating this integral are discussed: A Monte Carlo method and the method by Facet Decomposition. The first is limited by round-off error whereas the second is limited by computer storage and CPU running time. The Facet Decomposition method is exact when S is flat, and is superior to the Monte Carlo method when S is only slightly curved according to a certain criterion.

20. DISTRIBUTION/AVAILABILITY OF ABSTRACT UNCLASSIFIED/UNLIMITED ☐ SAME AS RPT. ☒ DTIC USERS ☐	21. ABSTRACT SECURITY CLASSIFICATION UNCLASSIFIED
22a. NAME OF RESPONSIBLE INDIVIDUAL W. B. Gordon	22b. TELEPHONE NUMBER (Include Area Code) (202) 767-2399 22c. OFFICE SYMBOL Code 5310

DD FORM 1473, 83 APR EDITION OF 1 JAN 73 IS OBSOLETE.

SECURITY CLASSIFICATION OF THIS PAGE

CONTENTS

TWO METHODS FOR CALCULATING THE PHYSICAL OPTICS FIELD

1. INTRODUCTION

Given a plane wave incident on a reflecting surface S, the physical optics (PO) field scattered by S is given by

$$J = -\frac{k}{4\pi R}\int_S \exp[-i\ k(\xi-\omega)\cdot x]\ (\xi-\omega)\cdot\eta\ dA \tag{1}$$

where $k = 2\pi/\lambda$ is the wave number, R is the radar range, ξ is a unit vector perpendicular to the wave front pointing from the source to S, ω is the unit vector pointing from S to the field point (observer), x is the position vector of a general point on S, η is the unit normal to S, and dA is the infinitesimal element of area on S. Hence J is a dimensionless quantity, and if P_i is the incident field power on S, the power at the field point is given by $P = P_i|J|^2$.

We shall hereafter be concerned with the monostatic case $\xi = -\omega$, so that ignoring the range dependence in (1), the integral becomes

$$J = (1/\lambda)\int_S \exp[i\ 2k\ \omega\cdot x]\ \omega\cdot\eta\ dA\ . \tag{2}$$

The radar cross section σ is then related to J by

$$\sigma = 4\pi\ |J|^2\ . \tag{3}$$

The integral (2) is always taken over only the illuminated part of a surface, defined by the relation $\omega\cdot\eta \geq 0$.

Closed form expressions for (2) can be obtained in only a few very special cases, and the numerical evaluation of these integrals is difficult. However, in previous work [1] the author has shown that the double integral (2) over S can be reduced to a line integral over the boundary of S when S is flat. If, moreover, S is a polygonal plate this line integral can be further reduced to a close-form expression involving no integrations at all. The existence of simple closed-form formulas for polygonal plates motivates the facet decomposition method for calculating the PO field scattered by a curved surface S: the surface S is approximated by a collection of triangular facets, and the closed form scattering formula is applied to each facet. The closed-form scattering formulas for polygonal plates are reproduced here in Appendix A, with certain modifications which are necessary to insure the proper phasing between the various facets.

We shall also consider the numerical evaluation of (2) by means of a Monte Carlo method in which integrals of the form

Manuscript approved January 11, 1984.

(4) $$J = \int_S f(x)\, dA$$

are approximated by sums of the type

(5) $$\hat{J} = \frac{A}{N} \sum_{n=1}^{N} f(x_n)$$

where the x_i are a random sample of points from a uniform distribution on S. In theory, there is no limit on the accuracy of either method, but there are practical limits to their usefulness, and the relative merits of the two methods is a question of economics (cost), and is machine dependent.

The Monte Carlo method almost always requires the use of thousands of functional evaluations, even when S is flat, whereas the facet decomposition method can sometimes yield accurate results with only a few facets when S is only slightly curved. On the other hand, the Monte Carlo method runs very fast, the coding is simple, and the requirements for computer storage are minimal, whereas the facet decomposition method requires a large amount of storage. For example, when the so called "optimal" compiler is used with the TI ASC, one is not permitted to use an array with more than $2^{15} \approx 33{,}000$ elements, and this limit is attained when the number of facets exceeds 5000.

The only practical limitation to the Monte Carlo method appears to be round-off error, caused by finite word length. This appears to limit the number of sample points to a few tens of thousands for the ASC (which has a short word length), and this limit is reached long before one exceeds a reasonable cost limit for CPU time. The finite word length also affects the reliability of the facet decomposition method, but in another way. The scattering formula for triangles is of the form $(A+B+C)/\varepsilon$, where, for near normal incidence, ε and $(A+B+C)$ are small, while each of the terms A, B and C is on the order of unity. When this happens the resulting calculation may be greatly in error, and one has to exercise care in devising methods to detect the occurrence of such bad cases and make the proper adjustments. The facet decomposition method can also be expensive in CPU time since it requires 9 trigonometric function evaluations for each facet whereas the Monte Carlo method requires only two trigonometric function evaluations per sample point.

Hence, to summarize, the Monte Carlo method runs fast, but its accuracy is limited by round-off error. The facet decomposition method is sometimes more costly in computer running time, and is also limited by constraints on computer storage. However, the facet decomposition method is more accurate and economical when the surface S is only slightly curved. Both methods require a substantial amount of calculation (thousands of points or facets) when S is a "moderately" curved surface which contains only a few Fresnal zones.

Finally, we should remark that the theory of Physical Optics is a high frequency approximation to reality, and that the problem of determining when

PO theory yields physically valid results is different from the mathematical problem addressed in this report, viz., the accurate numerical calculation of the integral (2).

2. TRIANGULAR DECOMPOSITION

Letting $x = (x^1, x^2, x^3)$ denote a general position vector for points on S, the surface S is defined by a system of parametric equations.

$$x = x(u,v) \tag{6}$$

where (u,v) varies over a domain D in the Euclidean plane. We usually take D to be the unit disk $\{u^2 + v^2 \leq 1\}$, or the unit square $\{0 \leq u \leq 1, 0 \leq v \leq 1\}$, depending upon whether S has one or two boundary curves. In the former case the boundary curve of S is not necessarily a circle since (6) describes a deformation of D. In the latter case S is topologically equivalent to a cylinder. Geometrically, a cylinder is obtained by gluing together two opposite sides of a square. In analytic terms, this means that the parametric equations for a cylinder satisfy

$$x(u, 0) \equiv x(u, 1).$$

To obtain an approximation of S by a collection of facets, we triangulate D and then lift the triangles via (6). Once a triangularization is given, a finer triangularization is obtained by replacing each triangle by four smaller ones, as we now describe.

Triangles in the disk D are said to be boundary or interior, the former being triangles with two vertices on the boundary circle. Thus, in Figure 1, only triangle 1 is boundary (since 2 has only one vertex on the boundary). To subdivide an interior triangle, we join the midpoints of the legs, as shown by the dotted lines in the figure. The subdivision of a boundary triangle is also shown in Figure 1, where A′ is the midpoint of the arc BC. Note that in subdividing a boundary triangle, we obtain two interior and two boundary triangles, and that only one of these four is contained in the original triangle.

To triangulate the disk D we first start with an initial configuration of F_o triangles obtained by joining F_o equispaced points on the boundary circle to the center. Figure 2a shows the initial configuration for the case $F_o = 4$, and it is seen that all the triangles in the initial configuration are of boundary type. Figure 2b shows the results of the first subdivision; there are 16 triangles, and in this case only the odd numbered ones are of the boundary type. At the second subdivision (not shown) there will be 64 triangles, of which only 16 will be of the boundary type. More generally, at each subdivision the total number F of triangles (or facets) increases by a factor of 4, while the number of boundary triangles doubles.

The initial configuration of a square is always taken to be the four triangles shown in Figure 3A. In this case we do not have to distinguish between boundary and interior triangles; at each subdivision each triangle is decomposed into four smaller ones by joining the midpoints.

Given a configuration of F triangles, let E, and V denote the number of edges and vertices, and let V_b be the number of vertices which lie on the boundary. Then, from topological generalities it is known that

$$F - E + V = 1,$$

$$2E = 3F + V_b \quad .$$

Hence, for F large, we have the approximate relations

$$E \approx (3/2)\, F \ ,$$

$$V \approx (1/2)\, F \ .$$

Table 1 shows the values of F, E, V, V_b for up to 5 subdivisions and two initial configurations. The row labled 0 shows the data for the initial configuration. Also, when D is the disk, V_b is also the number of boundary triangles.

TABLE 1

Values of F, E, V and V_b vs
Number of Iterated Subdivisions

Number of Iterations	$F_o = 3$				$F_o = 4$			
	F	E	V	V_b	F	E	V	V_b
0	3	6	4	3	4	8	5	4
1	12	21	10	6	16	28	13	8
2	48	78	31	12	64	104	41	16
3	192	300	109	24	256	400	145	32
4	768	1176	409	48	1024	1568	545	64
5	3072	4656	1585	96	4096	6208	2113	128

3. THEORETICAL ERROR ANALYSIS

3A. ERROR ANALYSIS FOR THE MONTE CARLO METHOD

To begin, given a general integral of type (4) we first calculate the standard deviation of the estimate (5). The derivation is given in Appendix B, and it turns out that $\hat{J}$ is an unbiased estimate of J whose standard deviation δJ is given by

$$\delta J = \frac{1}{\sqrt{N}} \left[A \int_S |f|^2 \, dA - |J|^2 \right]^{1/2} , \tag{7}$$

where A is the area of S. It is interesting to note that from the Schwarz inequality we have

$$|J|^2 = \left| \int f \cdot 1 \, dA \right|^2 \leq \int |f|^2 \int 1 \, dA = A \int |f|^2 \, dA \ ,$$

with equality only when f is constant; hence the term in brackets measures the variability of f.

In practice, the integral (2) over S is reduced to an integral over some planar domain, (e.g., by means of the parametric representation (6) discussed in the previous section), and an especially revealing relation is obtained if the plane P is perpendicular to the vector ω. We recall that the scattering integral is performed over only the illuminated portion of a surface for which $\omega \cdot \eta \geq 0$, and we have

$$dA_o = (\omega \cdot \eta) \, dA$$

where dA_o is the projection of dA onto P. Hence from (2),

$$J = \int_{S_o} (1/\lambda) \exp[i2k \, \omega \cdot x] \, dA_o \tag{8}$$

where S_o is the projection of S onto P. Applying (7) to the integral (8), we have $|f| = 1/\lambda$, and therefore

$$\delta J = \frac{1}{\sqrt{N}} \left[\frac{A_o^2}{\lambda^2} - |J|^2 \right]^{1/2} \ , \tag{9}$$

where A_o is the area of S_o. Setting

$$\sigma_o = 4\pi \, A_o^2/\lambda^2 \ , \tag{10}$$

from (8) we have $|J| \leq A_o/\lambda$, and from (3) we have

$$\sigma \leq \sigma_o \ , \tag{11}$$

and from (9) we have

$$\delta J = \frac{\sqrt{\sigma_o - \sigma}}{\sqrt{4\pi \, N}} \ . \tag{12}$$

We note that $\sigma = \sigma_o$ only when S is flat and the incidence is normal.

Following (3) it is natural to estimate the radar cross section σ by $\hat{\sigma}$ where

$$\hat{\sigma} = 4\pi \, |\hat{J}|^2 \ . \tag{13}$$

In Appendix B it is shown that $\hat{\sigma}$ has a bias B given by

(14) $$B(\hat{\sigma}) = (\sigma_o - \sigma)/N \ .$$

The general expression for the standard deviation $\delta\sigma$ of $\hat{\sigma}$ is extremely messy; however, when $\sigma << \sigma_o$ and the errors are small we have the approximate relation

(15) $$\delta\sigma/\sigma \approx \sqrt{2/N} \ \sqrt{\sigma_o/\sigma} \ .$$

Examples will be given in Section 3, and it will be seen that accurate estimates are harder to attain when σ is small.

B. Error Analysis for the Facet Decomposition Method

Let R_1, R_2 be the principal radii of curvature on S and let R_o be a lower bound to R_1, R_2 which holds everywhere on S. In Appendix C it is shown that when the total area of the collection of facets approximates the area of S, then the error ΔJ in the estimate of J satisfies

(16) $$\Delta J \leq \frac{8\pi}{\sqrt{3}} \cdot \frac{A^2}{\lambda^2 R_o} \cdot \frac{1}{N} \ .$$

and for small errors the corresponding bound for the relative error $\Delta\sigma/\sigma$ is

(17) $$\Delta\sigma/\sigma \leq \frac{32\pi^{3/2}}{\sqrt{3}} \cdot \frac{A^2}{\lambda^2 R_o \sqrt{\sigma}} \cdot \frac{1}{N} \ .$$

In particular, when S is flat, $R_o = \infty$, and the right hand sides of (16) and (17) are zero. Strictly speaking, these relations are derived only for the case when the facets are equilateral triangles; however, we have found that these relations are valid in the more general case, except when both the actual and predicted relative errors are extremely small ($<< 10^{-3}$). However, the error bound (17) is very often overly pessimistic, and we shall therefore discuss how the accuracy of the Facet Decomposition method can be judged by observing how the estimates vary with N.

4. EXAMPLES

In this section we shall present the results of numerical calculations for two test cases, the sphere and the spherical cap. In both cases we shall compare the results of the Monte Carlo and Facet Decomposition methods with each other, and with the performance predicted by the error analysis discussed in the previous section.

4A. The Sphere

We first consider the results for the Monte Carlo method. For a sphere of radius a, the illuminated part is a hemisphere with area $A = 2\pi a^2$, and the planar projection S_o has area $A_o = \pi a^2$. Hence

$$\sigma_o = (4\pi/\lambda^2)\ (\pi a^2)^2 \ .$$

When $ka > 1$, we have $\sigma \approx \pi a^2 << \sigma_o$, and from (14) and (15) we have

$$B = \frac{4\pi^3 a^4}{\lambda^2 N} \quad , \tag{18}$$

$$\delta\sigma/\sigma = ka\sqrt{2/N} \quad . \tag{19}$$

In the cases considered below, we take $a = 1$ and $\lambda = 1, 1/2, 1/4, 1/8$. For these cases we have $\sigma = \pi$ exactly, and in Tables 2-5 the columns labelled $\hat{\sigma}'$ are the estimated values of the normalized rcs $\sigma' = \sigma/\pi a^2$ ($=1$) obtained by a Monte Carlo approximation with the indicated number N of points, and B' and $\delta\sigma/\sigma$ are calculated according to

$$B' = \frac{4\pi^2}{\lambda^2 N} \quad ,$$

$$\delta\sigma/\sigma = \frac{(2\sqrt{2})\pi}{\lambda\sqrt{N}} \quad .$$

When $\delta\sigma/\sigma > 1$, the error is large and the results are unreliable. Since the true value of σ' is unity, the relative error is $|\hat{\sigma}' - 1|$, and we note that the errors always fall within the expected range. We also note that the errors would not be significantly improved by making the obvious bias correction.

We now consider the results for the Facet Decomposition Method. By convention, we take the parametrizing disc D to lie in the equatorial plane, and the entire sphere is triangulated by lifting the triangularization of the disc onto both the northern and southern hemispheres. As the aspect angle is varied different hemispheres are illuminated, and hence different aspect angles correspond in effect to different triangularizations of a hemisphere.

The results of the calculation are shown in Tables 6-9 for four different aspect angles θ, with θ being the colatitude, and three different levels of triangularization. The inital configuration (on the disc) was four triangles, and we show the results for the 3'rd, 4'th, and 5'th iterated subdivisions, with the number N of facets being 256, 1024, and 4096, respectively. (cf. Table 1.) The error bounds for $\Delta\sigma/\sigma$ given by (17) are not useful for these cases since they are all greater than unity, except for the case $\lambda = 1.0$, $N = 4096$ when the value is .56.

Confining our attention to the column $N = 4096$, we see that there are some particularly bad results at ($\lambda = 0.5$, $\theta = 90°$); ($\lambda = 0.25$, $\theta = 90°$); ($\lambda = 0.125$, $\theta = 0°$). In fact, in the first of these cases the results are better at $N = 1024$ than $N = 4096$.) In Section 1 we discussed a numerical problem which can occur when the incidence is almost normal to a facet, and the computer was programmed to treat near normal incidence as normal incidence, and to print a warning if the contribution from a facet was larger

TABLES 2-5

Monte Carlo Estimates of the Normalized RCS σ'
for the Unit Sphere

Table 2

$\lambda = 1.0$

N	$\hat{\sigma}'$	B'	$\delta\sigma/\sigma$
1200	1.0523	.0329	.26
4800	.8903	.0082	.13
19200	.9519	.0021	.064
38400	.9686	.0010	.045

Table 4

$\lambda = 0.25$

N	$\hat{\sigma}'$	B'	$\delta\sigma/\sigma$
1200	1.8505	.5264	> 1
4800	1.7256	.1316	.51
19200	.7201	.0329	.26
38400	.8137	.0164	.18

Table 3

$\lambda = 0.5$

N	$\hat{\sigma}'$	B'	$\delta\sigma/\sigma$
1200	.5779	.1316	.51
4800	1.1409	.0329	.26
19200	1.0215	.0082	.13
38400	1.0794	.0041	.091

Table 5

$\lambda = .125$

N	$\hat{\sigma}'$	B'	$\delta\sigma/\sigma$
1200	4.6054	2.1055	> 1
4800	3.3170	.5264	> 1
19200	1.2680	.1316	.51
38400	1.1914	.0658	.36

TABLES 6-9

Facet Decomposition Estimates of the Normalized RCS σ' for the Unit Sphere

Table 6

$\lambda = 1.0$

θ \ N	256	1024	4096
0°	1.0485	1.0826	1.0442
30	1.0186	.9184	.9402
60	.9534	.9870	1.0132
90	.2198	.6261	.9726

Table 8

$\lambda = .25$

θ \ N	256	1024	4096
0°	.1441	.7604	1.1206
30	.3090	.7550	1.0431
60	.8500	.8029	.9863
90	.6208	.2749	.5387

Table 7

$\lambda = 0.5$

θ \ N	256	1024	4096
0°	.6975	1.1027	1.0957
30	.7164	.8782	.9605
60	.9127	.8558	.9326
90	.0956	.9905	.5570

Table 9

$\lambda = .125$

θ \ N	256	1024	4096
0°	.0300	.0245	.7915
30	.2246	1.0458	1.0154
60	.8220	1.0939	.9315
90	1.1214	.7421	.9890

than theory permits. Such warnings did not occur, and since the worst (and best) results did not always occur at the same aspect angle, we do not believe that this numerical problem was responsible for these bad results. Because of the existence of these bad cases, we cannot claim that the Facet Decomposition method is superior to the Monte Carlo method for calculating the field scattered by a sphere.

4B. The Spherical Cap

Given a sphere of radius a, the surface area A and the projected planar area A_o are given by

$$A = 2\pi ah \quad ,$$

$$A_o = \pi r^2 = \pi (2ah - h^2) \quad .$$

(See Figure 4.) In the example we shall keep A and λ fixed, with $A = 2\pi$ and $\lambda = 1/8$, and we shall vary a in such a manner that h is an integral multiple of $\lambda/4$. Since $A = 2\pi ah = 2\pi$, we have

$$h = m\ \lambda/4 = m/32 \quad ,$$

$$a = 1/h = 32/m \quad .$$

We shall only present the results for axial incidence (along the axis of symmetry), and hence m is the number of Fresnel zones contained in each cap. One would therefore expect that σ is small when m is even, and this turns out to be the case. Although the Fresnel zones within a given cap have equal areas, σ is not exactly zero when m is even because of the "obliquity factor" $\cos\theta = \omega \cdot \eta$ occurring in the integrand (2).

The results of the numerical calculations are shown in Table 10 for both the Monte Carlo method with 40,000 sample points and the Facet Decomposition method with 4096 facets. The values of σ are shown in both absolute terms and dB, and the standard deviations $\delta\sigma$ and error bounds $\Delta\sigma$ are calculated according to (15) and (17), where σ is given the estimated value $\hat{\sigma}$ (unlike the case for the sphere, where the "true" value of σ was known and used). The value of σ_o is calculated according to (10), so that $\sigma_o = 31750$ (45.0 dB). We also recall that σ_o is the limiting value of σ as a increases without bound, and it was observed that for large values of a (not shown in the table), the estimated values of σ converged to this value.

We note that for m odd (and σ large), the Monte Carlo and Facet Decomposition estimates are within a few tenths of a dB of each other (except when $m = 9$), and that the two values always differ by less than $\delta\sigma$.

For even values of m (σ small), it appears that the Facet Decomposition method gives better results. The nulls predicted by this method are deeper than those predicted by the Monte Carlo method, and one would except to see extremely small values of σ when m is small and even. Moreover, the bias of the Monte Carlo method (calculated according to (14)) is equal to .79, which is larger than any of the estimated values of σ for m even, and the values of $\delta\sigma$ are also larger than $\hat{\sigma}$, so that the Monte Carlo estimates

TABLE 10

Monte Carlo and Facet Decomposition Estimates of $\hat{\sigma}$ for a Spherical Cap with Radius a and Height $h = m\lambda/4$. ($\lambda = 0.125$)

		Monte Carlo N = 40,000			Facet Decomposition N = 4096		
m	a	$\hat{\sigma}$	$\hat{\sigma}$ (dB)	$\delta\sigma$	$\hat{\sigma}$	$\hat{\sigma}$ (dB)	$\Delta\sigma$
1	32.0	12814.0	41.1	110.3	12764.0	41.1	224.0
3	10.7	1375.5	31.4	45.7	1412.7	31.5	222.9
5	6.4	525.8	27.2	28.6	499.9	27.0	221.7
7	4.6	236.2	23.7	19.3	250.4	24.0	218.3
9	3.6	124.6	21.0	14.0	146.6	21.7	213.5
11	2.9	88.4	19.5	11.8	94.6	19.8	212.9
2	16.0	.6441	-1.9	1.01	.0001	-40.0	0.04
4	8.0	.7228	-1.4	1.07	.0308	-15.1	1.39
6	5.3	.4908	-3.1	.88	.1186	-9.3	4.12
8	4.0	.1413	-8.5	.47	.2206	-6.6	7.45
10	3.2	.4912	-3.1	.88	.3360	-4.7	11.50
12	2.7	.5935	-2.3	.97	.4690	-3.3	16.10

are unreliable. We also note that for m even and increasing the Facet Decomposition estimates also increase, which is what one would expect because of the variation of the obliquity factor.

We again emphasize a distinction between (15) and (17). The first is an equation for the standard deviation of an estimate involving random factors, whereas the second is an upper bound to the error in an estimate involving no random quantities. A large value of $\delta\sigma/\sigma$ calculated according to (15) necessarily implies that the Monte Carlo estimate is unreliable, whereas a large value for the bound on $\Delta\sigma/\sigma$ given by (17) carries no such implication for the Facet Decomposition estimate. However, when the bound for $\Delta\sigma/\sigma$ is large the accuracy of the Facet Decomposition method can be judged by observing the variation of $\hat{\sigma}$ with increasing N. In Table 11 we have tabulated $\hat{\sigma}$ vs. N for 4 odd values and 4 even values of m. The estimates for m = 1, 5, 9 appear to be highly reliable since the values for N = 1024 and N = 4096 differ by less than one percent. We recall that the radius

TABLE 11

Facet Decomposition Values of $\hat{\sigma}$ vs. N = Number of Facets

	a = 32	a = 6.4	a = 3.6	a = 2.9	a = 16	a = 5.3	a = 3.2	a = 2.7
N	m = 1	m = 5	m = 9	m = 11	m = 2	m = 6	m = 10	m = 12
4	7323	206.8	59.69	38.29	1298.5	139.8	47.2	31.3
16	11801	344.4	26.74	57.45	222.7	223.9	46.8	7.0
64	12581	580.4	180.17	134.39	7.9	9.2	16.8	26.1
256	12746	473.8	164.44	112.48	.4472	.8577	4.7	2.4
1024	12795	498.2	147.11	98.51	.0321	.0921	.3730	.2126
4096	12764	499.9	146.63	94.63	.0001	.1186	.3360	.4690

$a = 32/m$ decreases as m increases, and we note that acceptable results are obtained for the largest value of a (flatest cap) with only 64 facets. For the even values of m, we note a large percentage difference between the values for N = 1024 and N = 4096, and it therefore appears that the relative errors are large. However, in absolute terms, one can still feel confident that $\sigma < 1$ in these cases, and hence that by introducing small (quarter-wavelength) changes in the height of a spherical cap can increase or decrease its rcs by orders of magnitude.

5. SUMMARY AND CONCLUSIONS

(i) The accuracy of the Monte Carlo method is limited by roundoff error, whereas the Facet Decomposition method is limited by computer storage and CPU time. The Facet Decomposition method is superior when the reflecting surface S is sufficiently flat.

(ii) The Monte Carlo estimate of σ has a bias B and standard deviation $\delta\sigma$ given by

$$B = (\sigma_o - \sigma)/N \quad , \tag{14}$$

$$\delta\sigma/\sigma = \sqrt{2/N} \quad \sqrt{\sigma_o/\sigma} \tag{15}$$

where N is the number of sample points, and

$$\sigma_o = 4\pi A_o/\lambda^2 \quad , \tag{10}$$

where A_o is the area of the projection of S onto a plane perpendicular to the incidence vector. An upper bound to the error of the Facet Decomposition method is given by

$$\Delta\sigma/\sigma \leq \frac{32\pi^{3/2}}{\sqrt{3}} \cdot \frac{A^2}{\lambda^2 R_o \sqrt{\sigma}} \cdot \frac{1}{N} \quad , \tag{17}$$

where N is the number of facets and R_o is a lower bound to the principal radii of curvature. (Thus $R_o = \infty$ when S is flat, in which case the Facet Decomposition method is exact.) According to these formulas, the calculation of σ should be easier and more reliable when σ, λ, and R_o are "large", and this prediction has been borne out by experience.

(iii) A large value of $\delta\sigma/\sigma$ (calculated according to (15) necessarily implies that the Monte Carlo estimate is unreliable, whereas a large value for the bound on $\Delta\sigma/\sigma$ given by (17) carries no such implication for the Facet Decomposition estimate. However, when this bound is large, one can still gauge the accuracy of the Facet Decomposition estimate by observing how it varies with increasing N, since accurate estimates will converge to some value (the true one) as N increases.

6. REFERENCES

[1] W.B. Gordon, Far field approximations to the Kirchhoff-Helmholtz representations of scattered fields, IEEE Trans. Ant. Prop. AP-23 (1975), P. 590-592.

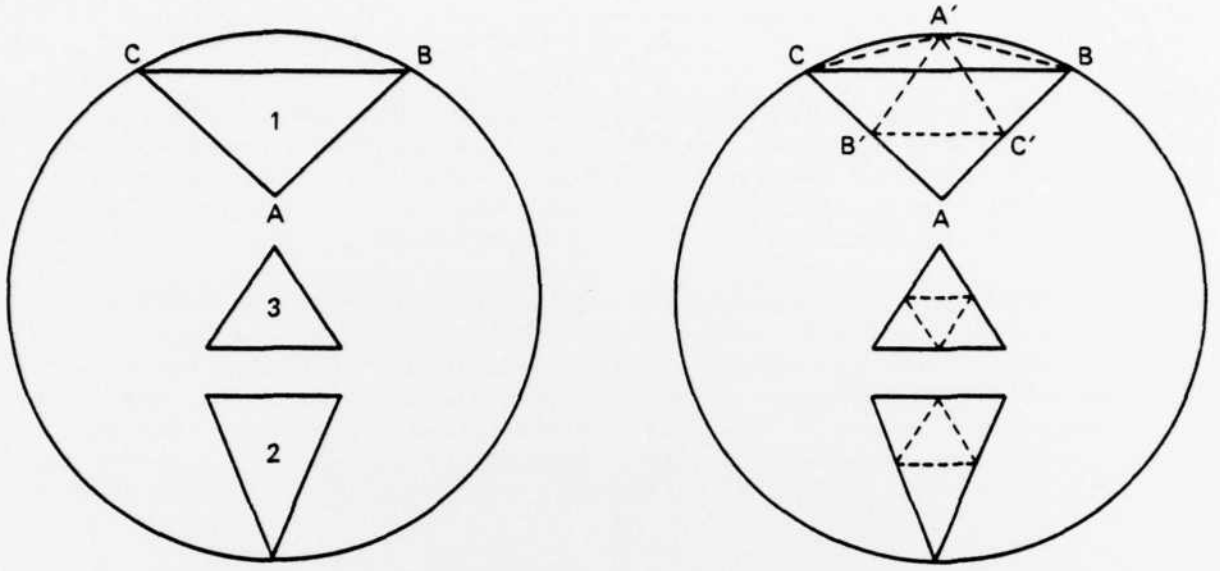

Fig. 1 — Subdivision of interior and boundary triangles
only the upper triangle (ABC) is of the boundary type

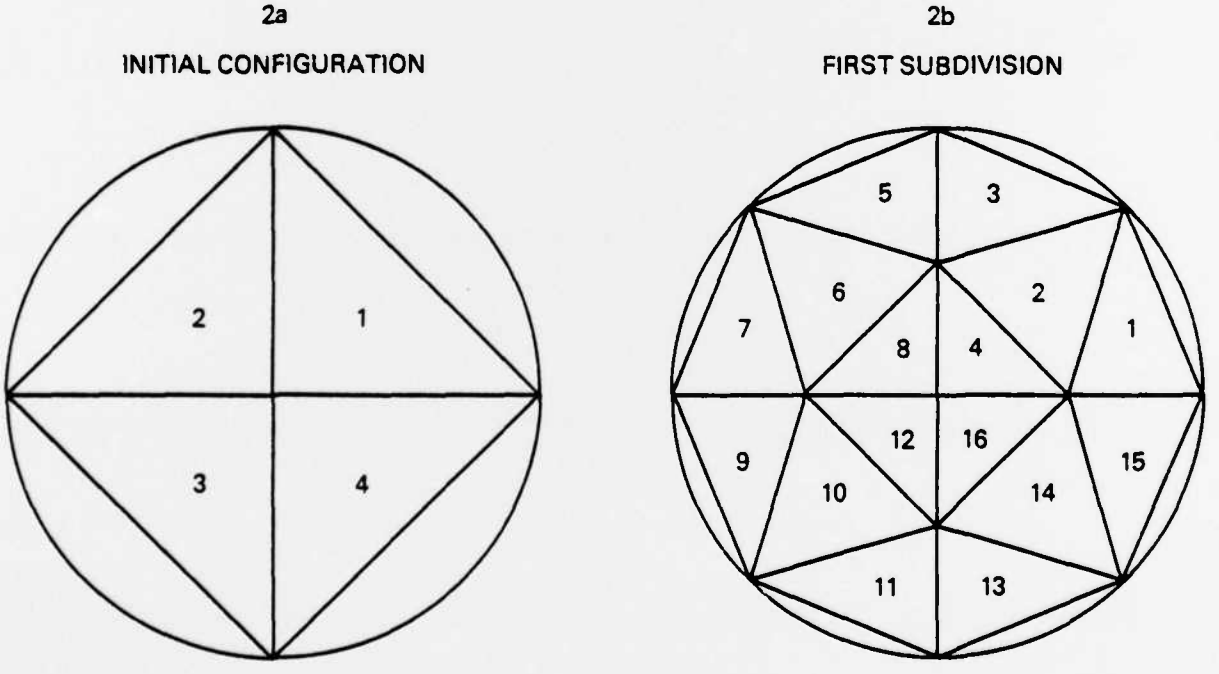

Fig. 2 — Subdivision of the disc

3a

INITIAL CONFIGURATION

3b

FIRST SUBDIVISION

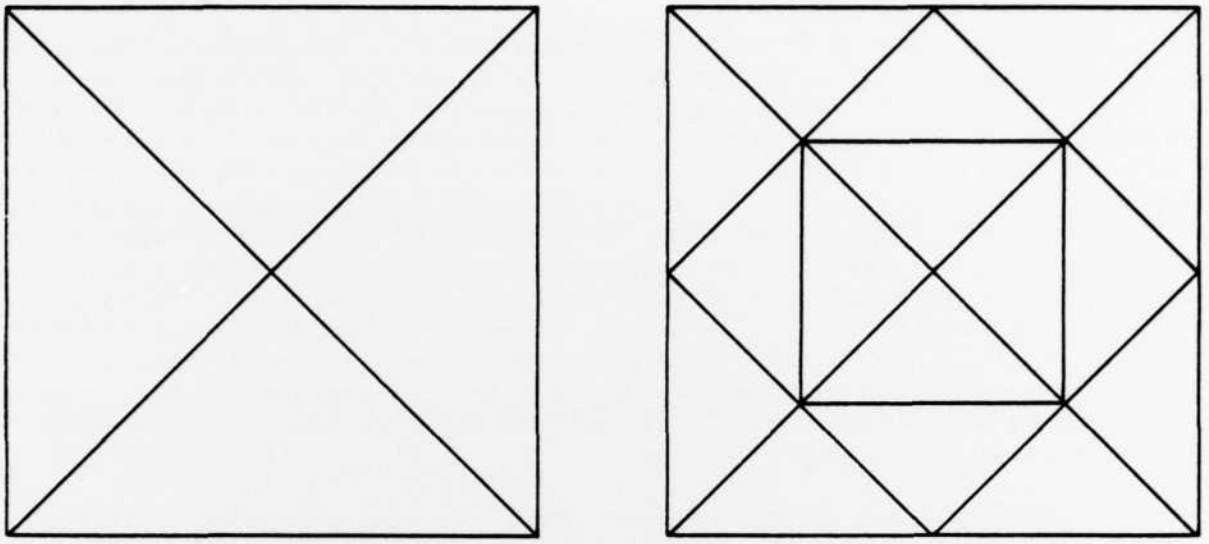

Fig. 3 — Subdivision of the square

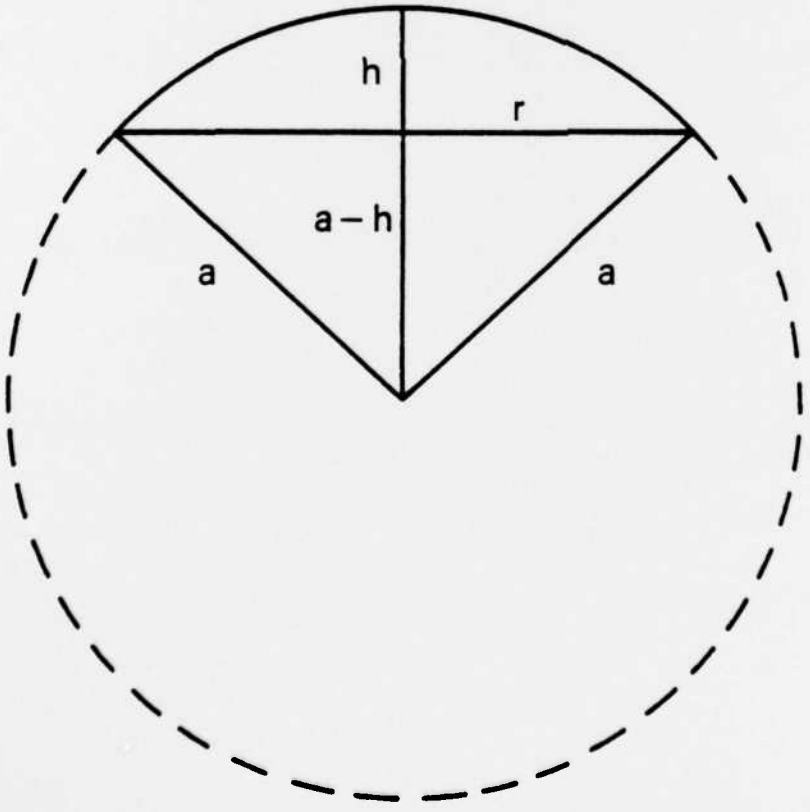

$$A = 2\pi ah$$
$$A_o = \pi r^2$$

$$r^2 = a^2 - (a-h)^2$$
$$= 2ah - h^2$$

Fig. 4 — Spherical cap with height = h

APPENDIX A

Scattering Formula for a Flat Polygonal Plate

In Ref [1] we gave a closed form expression for the Physical Optics (PO) field scattered by a flat polygonal plate, and for convenience the point of zero reference phase was chosen to lie somewhere on the polygon. In our present work we are concerned with summing the contributions from many different facets, and their relative phases must now be taken into account. A convenient way of doing this is to take the point of zero reference phase to be the field point, and to refer the vertices of all the polygons to a common coordinate system. (It might be "natural" to assume that the phase of the field scattered by each facet corresponds to its centroid, but this is not correct.) To obtain the correct result, we multiply the expression for the incident field (given at the bottom of p. 590 of Ref [1]) by a certain quantity ($\exp[-ik\,\xi \cdot R]$) which makes the phase zero at the field point. Then, by linearity, we multiply all the expressions given in Ref. [1] for the scattered field by the same quantity.

We shall give the resulting equations for a flat polygonal plate with N vertices. The results will be stated for the bistatic case, and we use the same notation as in equation (1) of Section 1 of this report. In addition, let

$\tilde{O}$ = fixed origin (same for all facets)

f = position vector of the field point P;

i.e., $f = P - \tilde{O}$.

x_n = position vector of the n'th vertex of the polygon.

$\alpha = \xi - \omega$ ($= -2\omega$ for the monostatic case)

$\beta = \alpha - (\alpha \cdot \eta)\,\eta$.

We set $x_{N+1} = x_1$ and $\Delta x_n = x_{n+1} - x_n$, $(n = 1, 2, \ldots, N)$. The field J scattered by the polygon is given by

<u>For $\beta \neq 0$,</u>

$$(4\pi R)\, J = \left[-\exp(-ik\alpha \cdot f)\right] \cdot \left[\frac{\alpha \cdot \eta}{|\beta|^2}\right] \cdot \sum_{n=1}^{N} T_n \quad ,$$

where

$$T_n = \left[(\alpha \times \eta)\right] \cdot \Delta x_n \cdot \left[\frac{\sin(\frac{k}{2}\,\alpha \cdot \Delta x_n)}{(\frac{k}{2}\,\alpha \cdot \Delta x_n)}\right] \cdot \exp\left\{\frac{ik}{2}\,\alpha \cdot (x_n + x_{n+1})\right\} \quad .$$

For $\beta = 0$,

$$(4\pi R)\, J = [-\exp(-ik\alpha\cdot f)]\,[2ik\,(\omega\cdot\eta)\,A\exp(ik\alpha\cdot q)]$$

where A is the area of the polygon and q is the position vector of any point on the polygon. (When $\beta = 0$, α is a scalar multiple of the normal vector η, and hence $\alpha\cdot(q-q') = 0$ for any two points q, q′ on the polygon.)

We note that the factor $[-\exp(-ik\,\alpha\cdot f)]$ is the same for all facets, and hence can be neglected when the total set of scatterers consists of polygons only.

APPENDIX B

Error Analysis for the Monte Carlo Method

Let x be a random point with a uniform distribution on S, and let f be a function on S with integral

$$J = \int_S f \, dA \quad .$$

The expected value of f(x) is

$$E\, f(x) = \int f(x) \frac{dA}{A} = J/A$$

since dA/A is the uniform density on S. Hence the quantity A f(x) is an unbiased estimator of J, and its variance is

$$E[|A\, f(x)|^2] - |J|^2 = \int A^2 |f|^2 \left(\frac{dA}{A}\right) - |J|^2$$

$$= \int A|f|^2 \, dA - |J|^2 \quad .$$

The relation (7) then follows from (5), since the quantities A $f(x_n)$ are uncorrelated estimates of J.

The calculation of the standard deviation δJ is given in the text. To calculate the bias B, let ΔJ be the error in $\hat{J}$. Then

$$\hat{\sigma} = 4\pi \, |\hat{J}|^2 = 4\pi \, |J + \Delta J|^2 \quad .$$

Expanding, and using the fact that $E(\Delta J) = 0$ (since J is unbiased), we get

$$E\hat{\sigma} = 4\pi[|J|^2 + E\,|\Delta J|^2] = \sigma + 4\pi \, |\delta J|^2 \quad .$$

Hence, using (12),

$$B = E\hat{\sigma} - \sigma = 4\pi |\delta J|^2 = (\sigma_o - \sigma)/N \quad .$$

We conclude by sketching the derivation of (15). Let J_1 and J_2 be the real imaginary parts of J, so that

$$\sigma = 4\pi(J_1^2 + J_2^2) \quad .$$

Then, neglecting higher order terms for small errors, we have

$$\Delta\sigma = 8\pi \, (J_1 \, \Delta J_1 + J_2 \, \Delta J_2) \quad .$$

Squaring, and applying the expected value operator E, we get

$$(\delta\sigma)^2 = E(\Delta\sigma)^2 = (8\pi)^2 \left[J_1{}^2(\delta J_1)^2 + (J_2)^2(\delta J_2)^2 + 2J_1J_2E(\Delta J_1 \cdot \Delta J_2\right] .$$

If one writes out the errors $(\Delta J_1)^2$, $(\Delta J_2)^2$ and the corresponding expressions for the variances $(\delta J_1)^2$, $(\delta J_2)^2$, then it turns out that some terms are on are on the order of σ_o/N while others are on the order of σ/N; neglecting the latter, one obtains

$$(\delta J_1)^2 = (\delta J_2)^2 \approx \frac{\sigma_o}{8\pi N} ,$$

$$E(\Delta J_1 \cdot \Delta J_2) \approx 0 .$$

Hence

$$(\delta\sigma)^2 = (8\pi)^2 \left(J_1{}^2 + J_2{}^2\right) \frac{\sigma_o}{8\pi N} = (8\pi)^2 \cdot \frac{\sigma}{4\pi} \cdot \frac{\sigma_o}{8\pi N}$$

$$= 2\ \sigma\ \sigma_o/N ,$$

and

$$\delta\sigma/\sigma = \sqrt{2/N}\ \sqrt{\sigma_o/\sigma} .$$

APPENDIX C

Derivation of the Error Bounds for Facet Decomposition

Let f denote the vector valued function

$$f(x) = \exp[i2k\omega \cdot x]\ \omega/\lambda \quad ,$$

so that

$$J = \int_S f \cdot \eta \, dA \quad .$$

Since $|\omega|^2 = 1$, the divergence of f is given by

$$\nabla \cdot f = (i2k/\lambda) \exp[i2k\omega \cdot x] \quad .$$

Hence, using the Divergence Theorem,

$$|\Delta J| = \left| \int_{\Delta V} \nabla \cdot f \, dV \right| \leq (4\pi/\lambda^2)\ \Delta V \quad ,$$

where ΔV is the volume contained between the surface S and the approximating collection of facets.

With a little geometry one can show that

$$\Delta V \leq h_o\ A \quad ,$$

where h_o is an upperbound to the height of any point on S above the nearest facet, and that

$$h_o \leq \frac{D^2}{2R_o} \quad ,$$

where D is an upperbound to the length of the facet edges. Hence

$$\Delta J \leq \frac{2\pi A}{\lambda^2 R_o} \cdot D^2 \quad .$$

If we now assume that the triangularization is so fine that the total area of the facets is approximately A, and that the triangles are equilateral, we have

$$N\left(\frac{\sqrt{3}}{4} D^2\right) = A \quad .$$

From these last two relations we get (16).

To derive (17) from (16) we use the usual first order approximations

for small errors. We have

$$\sigma = 4\pi\, J\, J^* \quad ,$$

$$\Delta\sigma \approx 4\pi\, (J\, \Delta J^* + J^*\, \Delta J) \quad .$$

Hence

$$\left| \frac{\Delta\sigma}{\sigma} \right| \approx \left| \frac{\Delta J^*}{J^*} \right| \leq 2\, \frac{|\Delta J|}{|J|} = 4\sqrt{\pi}\, \frac{|\Delta J|}{\sqrt{\sigma}} \quad .$$


MD
-84